Relazione Scientifica – Scientific Report
SUMMARY

Titolo del programma: Studio della risposta atmosferica al mescolamento dell'acque oceaniche dovuto alle maree nei mari del Maritime Continent (MC).

Proponente/Fruitore: Dr. G.L.Liberti. Ricercatore livello III, ISAC-CNR. UOS Roma.

Istituto di afferenza: Istituto Scienze dell'Atmosfera e del Clima

Dipartimento di afferenza. Scienze del sistema Terra e Tecnologie per l'Ambiente

Descrizione dettagliata dell'Istituzione ospitante: La Scripps Institution of Oceanography (https://scripps.ucsd.edu/about) e' un Dipartimento dell'University of California, San Diego (UCSD). E' uno dei centri più importanti, per dimensione, campi d'interesse e tradizione, per la ricerca, l'insegnamento e lo sviluppo di applicazioni nel campo delle scienze dell'oceanografia, la fisica dell'atmosfera e le scienze della terra. Tra le varie facilities possiede una flotta di 4 R/V e la piattaforma FLIP.

Obiettivi: A partire dalla conoscenza che, nei mari interni al Maritime Continent, il rimescolamento dovuto alle maree produce una variazione relativamente importante e dalle caratteristiche spaziali e temporali peculiari, della temperatura superficiale del mare (SST) si intende investigare l'ipotesi che l'atmosfera risponda a tali variazioni con un cambio nelle caratteristiche delle variabili legate al ciclo dell'acqua: vapor d'acqua, nubi e precipitazioni.

Descrizione del progetto: Il progetto unisce competenze, presenti all'ISAC-CNR relative alle tecniche di misura, in situ o da telerilevamento, delle variabili atmosferiche legate al ciclo dell'acqua e alla loro analisi a quelle relative alle tecniche di misura e interpretazione dei risultati per le variabili d'interesse di oceanografia fisica presenti nel laboratorio ospitante. A tali complementarità si aggiunge uno specifico interesse comune per la regione del MC documentato dalla produzione scientifica del fruitore e dell'ospite. La letteratura esistente ipotizza, nella regione, la possibilità di una relazione tra scale di variabilità spazio-temporale delle grandezze che descrivono il ciclo dell'acqua e le maree attraverso la variazione di SST dovuta al rimescolamento resa complessa dall'interazione con la batimetria e con le correnti. Il progetto si propone di verificare quantitativamente tale ipotesi e contribuendo alla caratterizzazione delle scale di variabilità atmosferica nella regione.

Motivi e valore aggiunto della richiesta: La proposta rientra nel quadro delle attività preparatorie la campagna internazionale 'Year of Maritime Continent' (www.bmkg.go.id/ymc/) per lo studio del ruolo del Maritime Continent (MC) su meteorologia e clima globale. Entrambe le strutture coinvolte nel progetto STM 2015 partecipano a tale campagna. La struttura ospitante possiede un know-how unico sull'oceanografia fisica dei mari dell'MC.

The atmospheric response to tidal mixing in the Indonesian Seas

1 Introduction

The Indonesian seas are sites of intense tidal energy (Figure 1) (Ffield and Gordon, 1996; Hatayama, 2004; Koch-Larrouy et al., 2007; 2008; Nagai and Hibiya, 2015). Because of the abruptly sloping topography resulting from the complex bathymetry of deep basins and shallow surrounding shelves, much of the dissipation of this tidal energy is trapped within the Indonesian seas and becomes available for vertical mixing (Schiller, 2004; Koch-Larrouy et al., 2007; Robertson and Ffield, 2005). The enhanced mixing acts to regulate air-sea interaction in the region via a number of different processes. The sea surface temperature (SST) is cooled by tidal mixing as colder deeper water is drawn up to the surface. Observations and the numerical models that parameterize tidal mixing show a direct affect on basin averaged SST by ~0.3°-1°C in the annual mean (Ffield and Gordon, 1996; Schiller, 2004; Koch-Larrouy et al., 2008; Kida and Wijffels, 2012). When the background SST ranges from 25°-30°C such as in the Indonesian seas, these cooler SST can reduce the latent heat flux to the atmosphere by 20-40 Wm^{-2} (Ffield and Gordon, 1996; Koch-Larrouy et al., 2008). In addition, given the proposed convective limit of SST at ~27°C (Graham and Barnett, 1987), it is expected that even small changes of SST in the region would significantly modify the frequency and intensity of tropical convection. Indeed, coupled simulations that include tidal parameterizations lead to a redistribution and improvement of the precipitation patterns compared to observations over the Indonesian seas (Jochem and Potemra, 2008; Koch-Larrouy et al., 2010). Not surprisingly, given that the ascending branch of the Walker Circulation lies over the Indonesian seas, these changes also lead to changes in the wind convergence that then feedback to impact the strength and variability of both the Pacific ENSO mode and the Indian Ocean Dipole mode (Koch-Larrouy et al., 2010). Finally, it has long been recognized that tidal mixing within the Indonesian seas likely plays a fundamental role in the water mass transformation of the Pacific waters (Ffield and Gordon, 1992; Hautala et al., 1996). Several recent numerical studies have confirmed that tidal mixing is required for this transformation to occur (Schiller 2004; Koch-Larrouy et al., 2007; Jochem and Potemra, 2008).

The spatial distribution of intense mixing sites appears to be highly variable within the Indonesian seas, although there are still precious few observations of direct mixing to verify this. Temperature-salinity profiles suggest Pacific water masses are transformed immediately upon entry into the Indonesian seas (Sprintall et al., 2014), and strong tidal mixing above sharp topography and in energetic narrow straits has been inferred from temperature profiles (Ffield and Robertson, 2005). More recently, the first direct measurements of turbulent dissipation in the Indonesian waters confirmed that enhanced dissipation energy occurs within these inflow and other straits [10^{-7}-10^{-5} W.kg^{-1}], in contrast to lower values within the deep basins far from the internal tide generation sites [10^{-11}-10^{-8} W.kg^{-1}] (Koch-Larrouy et al. 2015). Nonetheless, Ffield and Gordon (1996) suggest that on fortnightly to monthly periods the largest tidal mixing signatures occur away from the coasts, within the Seram and Banda Seas. Turbulent mixing at the inertial time scale has also been observed at the base of the mixed layer in the Banda Sea (Alford et al., 1999, 2001). The apparent discrepancy might partially be explained by recent model results that suggest the generation and dissipation sites of the internal tides responsible for water mass transformation may not necessarily coincide (Nagai and Hibiya, 2015). Thus it may be that SST response to tidal mixing might not be a localized phenomenon.

3

Since tidal forces are strongly time dependent, one might expect that any product of tidally-induced vertical mixing would display similar periodicities. For example, tides might result in a cycle of alternating cool to warm SST over the same period, respectively corresponding to the strong and weak vertical mixing phases of the tidal cycle (Loder and Garrett, 1978). Certainly there is an observed component in the SST periodicity in the Indonesian Seas that can be related to the tides. For example, a prominent fortnightly tidal signal in the SST is found within the internal Banda Sea (Ffield and Gordon, 1996), Makassar Strait (Ffield et al., 2000) and the outflow passages of Lombok and Ombai Straits (Sprintall et al., 2003). Because SST is a commonly measured geophysical variable whose variability depends on the exchange processes at the interface between the coupled air-sea system, one might also expect some type of related response in the atmospheric variability over tidal frequencies. As discussed above, model simulations that parameterize tidal mixing within the Indonesian seas result in cooler SSTs (0.5°-2°C) that lead to a 20% weaker convection, more aligned with the observed precipitation patterns (Jochem and Potemra, 2008; Koch-Larrouy et al., 2010). In general the largest precipitation changes are co-located with the SST changes, however again there may be significant non-local impacts in other global regions (Koch-Larrouy et al., 2010; Brierley and Federov, 2011). For these studies the atmospheric response appears in the model's annual mean state. Likewise, many studies have shown a link between the long-term modulation of the lunar ~18.6 year nodal cycle on the lunar diurnal and semidiurnal oceanic tides, which eventually can affect climate on similar bi-decadal time scales (Keeling and Whorf, 1997; Yasuda et al., 2006; Ray, 2007; McKinnell and Crawford, 2007 etc.). There is also a significant body of literature devoted to the effect of *atmospheric* tides and lunar forcing on surface air temperature and atmospheric circulation on fortnightly and longer time scales (e.g., Anyamba et al., 2000; Li et al., 2011 etc.). However atmospheric tides differ from oceanic tides: atmospheric tides are excited primarily by the sun heating the atmosphere, whereas ocean tides are excited primarily by the gravitational attractions of the moon and sun acting on the oceans. To our knowledge, the relationship of a direct atmospheric response to SST on shorter (sub-monthly) period oceanic tidal frequencies has not yet been reported.

The goal of this study is to seek observational evidence of a response in the atmospheric water vapour to the complex tidal mixing signature in the Indonesian seas, specifically in SST on fortnightly time scales. Our premise is that observed synchronicity seen at this 14-day periodicity argues sufficiently in favor of a tidal-forcing hypothesis to justify further investigation of a possible tidal mechanism of temperature and climate variability. The study builds on that of Ffield and Gordon (1996), who examined the influence of 14-30 day tidal cycle in the Indonesian seas using limited disparate data sets. While they speculated about a feedback of tidally induced SST variations to the atmospheric system, they did not directly investigate any sea-air linkages. With today's remotely sensed measurements of both the atmosphere and the SST it is now possible to undertake this effort. Specifically, the paper will address the science questions: What is the relevance of the air-sea interaction resulting from the 14-day spring-neap tides in the Indonesian region? What are the mechanisms that transfer the SST anomalies to the atmosphere? Potential candidates include (1) SST-induced changes in the evaporation rates, and/or (2) changes in the dynamical (convergence and stability) local atmospheric circulation.

The paper is organized as follows. A description of the remotely sensed and *in situ* data sets used in the study, along with a discussion of their relative suitability for the analysis, is found in section 2. Section 3 first discusses the challenges faced in isolating the tidal mixing signal from other potential mixing mechanisms, and then details our multi-pronged methodological approach to potentially isolate the tidal signal. Results are presented for selected single time-

series sites, as well as broader sub-regions of interest within the Indonesian seas. Finally, Section 5 summarizes and discusses the robustness of the results, and provides a perspective of our work.
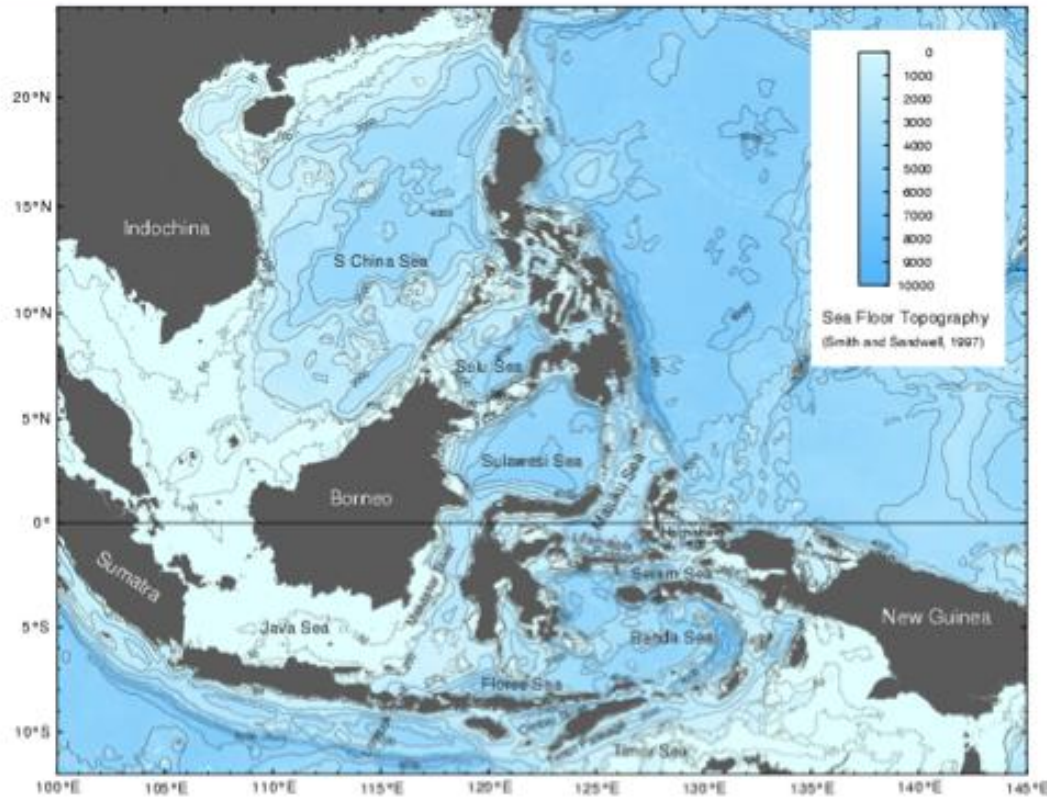

Figure 1: Sea floor Topography of Indonesian seas *(Smith and Sandwell, 1997)*

2   Data Sets

This section contains the description of the data sets used or planned to be used for the study. The area of interest for this study was is defined by the following latitude and longitude values 15°S-15°N, 90°E-155°E. This area include, the Indonesian Seas as well as part of the surrounding Oceans in order to have a reference information regarding the open Ocean area.

2.1 Remotely-sensed Data Sets(TMI)

This study takes advantage of remotely-sensed SST and Total Precipitable Water (TPW i.e., the column integrated Water Vapour) measured concurrently from the Tropical Rainfall Measuring Mission (TRMM) Microwave Imager (TMI). We use the TMI Version 7.1 products from December 1997-December 2014, available through Remote Sensing Systems (www.remss.com). For our study purposes, there are a number of advantages to using SST and WV measured from the same TMI sensor. Perhaps most fundamentally, the satellite is on a non-sun synchronous cycle, so the measurements resolve the daily cycle in the tropics, which is central to be able to detect our tidal signal. In addition, TPW is directly linked through evaporation to SST variability (e.g. Stephens 1990, Zhang & Qiu 2008, Kanemaru & Masunaga, 2013) and so in principle, any evident tidal signal in WV should be more robust than in the available remotely sensed cloud or precipitation measurements. Certainly TPW is a more continuous and relatively smooth variable compared to cloudiness and precipitation. Although typically coarser resolution than infrared measurements, microwave measurements

5

have the added distinct advantage of being able to retrieve data even under cloudy non precipitating conditions, which is particularly useful in the perpetually cloudy Indonesian seas. In addition, infrared radiometry SST measurements are of the skin temperature of the ocean surface, which has a larger sensitivity to wind and radiation signals that can potentially contaminate any tidal signal compared to microwave SST measurements. TPW can be measured in almost all conditions through microwave passive radiometry, although as an integrated quantity, if the SST-TPW interaction is relatively weak and very likely interacts only within the marine boundary layer then it may be difficult to isolate the signal. Finally, as well as SST and WV, the satellite also measures gives cloud liquid water, precipitation and wind at surface, which is particularly useful since determining SST from microwave measurements requires correction for sea surface roughness (due in part to wind) and atmospheric attenuation due to rain, water vapor, clouds, and oxygen (Wentz and Meissner, 2000). In addition, having concurrent measurements allows us to examine the relationship of SST to these variables over the same time and space scales.

All TMI retrieved geophysical variables are archived in daily files, mapped on a 0.25°x0.25° regular grid using an optimal interpolation scheme. For each grid point and variable, the daily files consist of two observations: one for the descending orbit and another for the ascending orbit. While more than two observations per day are possible for the TRMM orbit (because of the overlap between the first and the last orbit segments of the day, or because of the overlap between contiguous orbits when close to the upper and lower latitude TMI observing limits), only the latest values of the retrieved parameters are reported in the available files. Hence part of the diurnal sampling information potentially contained in the original TMI observations is lost.

Each geophysical variable is stored as a single byte using the values 0-250, with 251-255 reserved for quality flag indicators. For TPW, the range is set from 0 to 75 mm, with a numerical resolution of 0.3 mm. For SST, the range is -3 to 34.5 °C with a 0.15 °C numerical resolution.

The algorithm used to retrieve all geophysical parameters is described in Wentz and Meissner (2000; 2007). It was originally developed for SSMI (Wentz, 1997) and optimized for the TMI and AMSRE instruments, both of which have lower frequency channels (<19 Ghz) that are sensitive to SST. For TPW and cloud liquid water the 19, 22 and 37 Ghz channels are used. In brief, the inversion algorithm is based on a two-stage regression between brightness temperatures (T_b) and geophysical parameters, using ancillary information of wind direction from the NCEP-GDAS (National Centre for Environmental Prediction - Global Data Assimilation System) analysis, and salinity from the NODC (National Oceanographic Data Center) World Ocean Atlas (Antonov et al., 2010). All regression coefficients are obtained from a training set of T_b that originates from a set of geophysical realizations simulated using a Radiative Transfer Model. The geophysical realizations are generated using initial data from 42195 radiosonde profiles launched from weather ships or from 56 small island sites. Of these, 37650 radiosondes were launched between 1987 and 1990, with the remaining launched between 1990 and 2000. An ensemble of geophysical realizations were then created by perturbing each profile: cloud water varied from 0 to 0.3 mm; SST varied +/-5.5°C based on values from the Reynolds et al. (2007) climatology; wind speed varied from 0-40 ms^{-1} and the wind direction from 0-360° in 20° steps. Several studies have examined the TMI derived SST RSS products [e.g. Reynolds et al., 2010;]; however, TMI derived TPW remains relatively unexplored, with to our knowledge only two validation studies so far [Sajith et al., 2007; Liberti et al. 2012] that used previous versions of TMI distributed products.

While in presence of precipitation the SST is not retrieved, an estimation of TPW is given also in case of rain. In principle, in presence of precipitation, the capability of TMI to separate different contribution of atmospheric variables decreases. The comparison against radiosonde (Liberti et al. 2012) shows that the agreement between TMI and radiosonde estimated TPW decreases when cases with TMI detected precipitation are included in the comparison. In this study, in some cases we performed the analyses including or not the cases identified as precipitating in TMI observations.

Figures 2-4 shows the distribution of observations and some statistics for the SST and TPW (including or removing the precipitating cases). Similar statistics were computed (not shown) also for the other TMI derived variables (Surface wind, Cloud liquid water and precipitation). Note that the different distribution in available observations (NPT upper row left panel), beside the fact that TPW is retrieved also in case of precipitation, derive from the fact that SST retrieval is based on lower frequencies (larger Field of View) channels and therefore gridboxes closer to the coasts are more easily contaminated than for the TPW that is based on higher frequency channels.
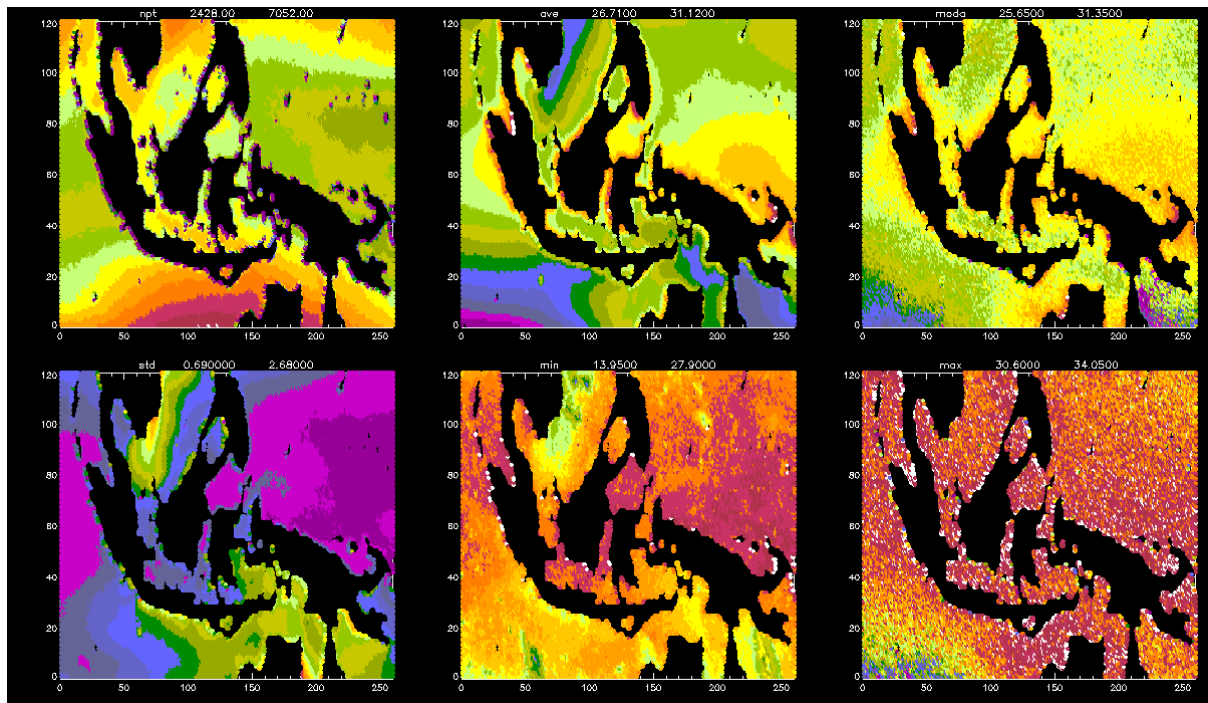

Fig.2. Overall statistics for the TMI derived SST. From left to right from upper to lower: **NPT:** Number of point. **AVE**: Average. **MODA**: Moda, **STD**: standard deviation, **min**: Minimun; **max**: Maximum. Associated colour scale is reported in Appendix 1. Minimum (Black) and Maximum (White) values are the ones reported in the title of each panel.
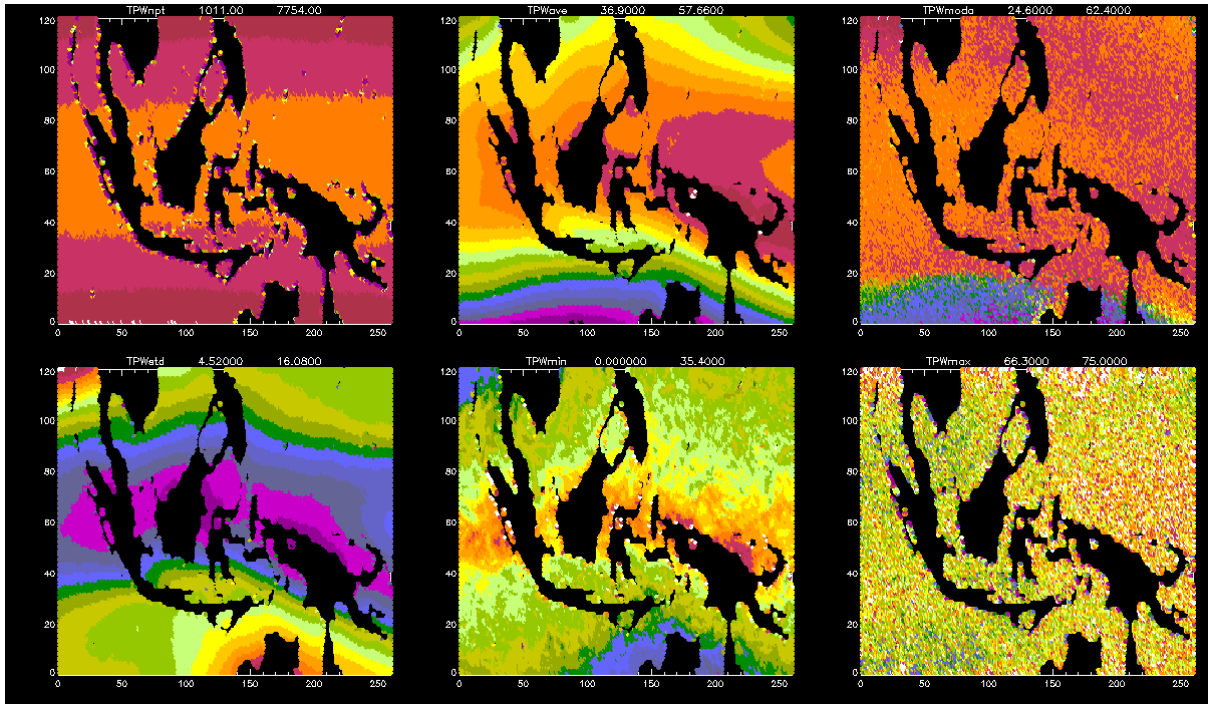
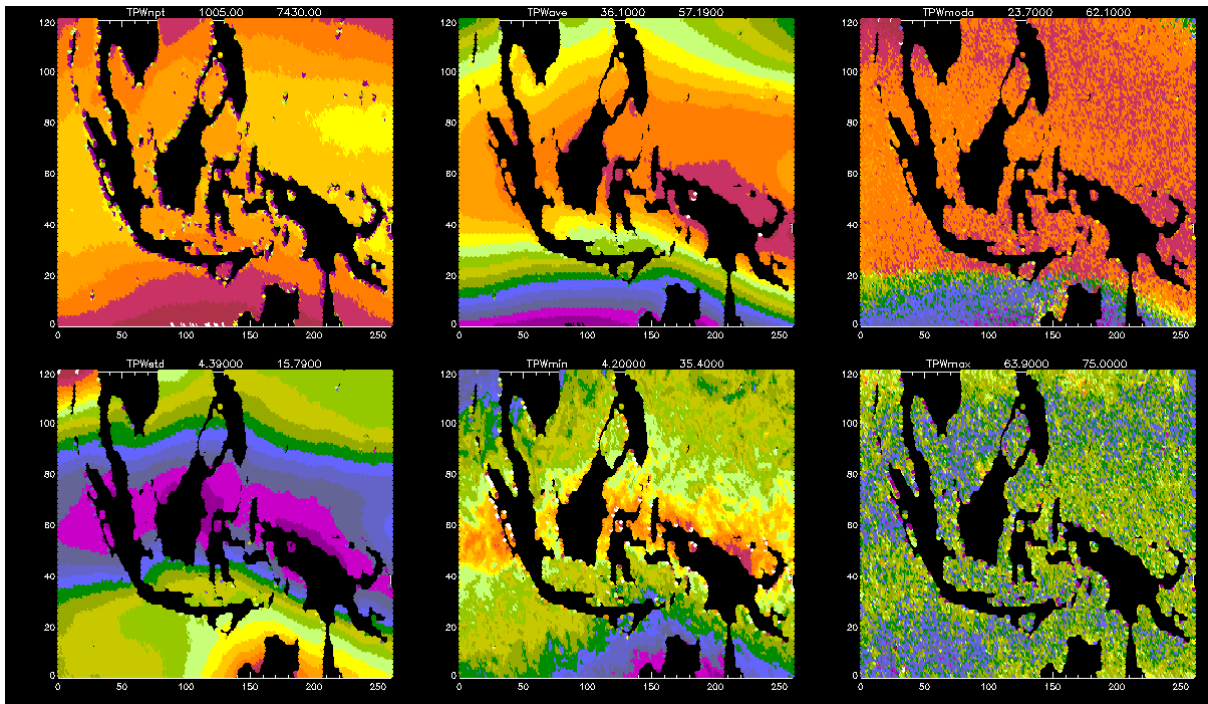**Fig.3.** As Fig.2 for the TMI derived TPW.

Fig.4. As Fig.2 for the TMI derived TPW for non precipitating cases only.

2.2 Operational Radiosonde Soundings

The TMI and other available passive MW derived estimation of TPW are able to give a description of its spatial variability in the study area, however as pointed out by several authors (REFS) the relationship between SST and TPW depends on the vertical distribution of WV. For this reason we also make use of atmospheric radiosonde profile measurements extracted from the Integrated Global Radiosonde Archive (IGRA, https://www.ncdc.noaa.gov/data-access/weather-balloon/integrated-global-radiosonde-

[archive](#)) that contains quality controlled radiosonde and pilot balloon observations at over 1500 globally distributed stations (Durre et al. 2006). These direct measurements began in the late 1940's and so provide a much longer time series than the remotely sensed measurements, although there may be some variability due to the change in radiosonde types and models over the years, and their dependence on solar radiation is not well documented. Typically radiosondes are routinely released twice a day from land-based stations, although there are a few cases where there are 4-8 launches per day. In the majority of cases, the information and sampling of the radiosondes contained in the IGRA archive are those originally sent through the Global Telecommunication System (GTS) of the World Meteorological Organization (WMO). The reported variables are pressure [Pa], geopotential height [m], air temperature [°C], Dew Point Depression (DPD) [°C], wind direction [°] and wind speed [m/s]. Air temperature and DPD are reported with a 0.1°C numerical discretization. Quality assurance flags are given for each pressure, geopotential height, and temperature value that indicates whether the corresponding value was checked using quality control procedures based on climatological means and standard deviations. In accordance with WMO guidance, the vertical sampling in the reported radiosonde profiles is given at standard pressure levels (1000, 925, 850, 700, 500, 400, 300, 250, 200, 150, 100, 70, 50, and 10 hPa), at the surface, at the tropopause and at significant thermodynamic and wind levels (WMO 1986). Metadata information on the archived radiosonde observations is available at the IGRA web site.

Several variables of interest from the radiosonde data are considered. *TPW* (mm) is computed as:

$$TPW = \frac{1}{\rho_w} \int_{psfc}^{0} \frac{w(p)}{g(p)} dp \qquad [1]$$

where *w(p)* is the specific humidity at the pressure level *p*; *g(p)* is the gravity acceleration; and ρ_w is the water density (1000 kg/m^3) needed to convert the integral [kg.m^{-2}] to [mm]. Radiosonde estimates of TPW (TPW$_{RDS}$) are obtained by computing the specific humidity for each level that has valid temperature, pressure and DPD measurements and then numerically integrating the specific humidity over the vertical profile according with the following formula:

$$TPW_{RDS} = \frac{1}{\rho_w} \sum_{i=1}^{NLEV} \frac{1}{g_i} \cdot \left(\frac{w_i \cdot p_i + w_{i-1} \cdot p_{i-1}}{p_i + p_{i-1}} \right) \cdot (p_i - p_{i-1}) \qquad [2]$$

where the gravity g_i is computed applying a two variables (latitude and altitude *h*) model (NIMA 1984). The altitude *h* is obtained from the pressure iteratively integrating the dry hydrostatic equation starting from a profile of g=9.8066 m s^{-2} and successively modifying the value of the gravity. The integration was performed with all valid levels up to 100 hPa. No correction for the contribution above this value was introduced. In this phase of the study all soundings with at least 5 valid levels were included in the analyzed dataset .

We also examine the *WV mixing ratio at the surface [g/kg]*. Our rationale here is that if the effect of the tidal mixing is largely confined to the surface layer then this variable will better respond to the tidal forcing while the integrated TPW quantity would tend to be dominated by larger scale processes. On the other hand we should take into account that radiosonde sites are over land and in some case not very close to the coast.

The Convective Available Potential Energy (CAPE) provides a measure of amount of energy (J/kg) that is available during convection, and is calculated by integrating vertically the local buoyancy of the parcel from the level of free convection to equilibrium level.

9

Finally, we also consider the surface pressure, which is directly related to WV (Trenberth et al., 1987).

Given the expected relevance of the vertical distribution of water vapour, the radiosonde processing included the computation of four different variables, expressed as a pressure value, aimed to contain the information of the WV vertical distribution.

- P_1: Scale height pressure defined as the pressure for which the specific humidity is

$$q(P_1) = q(P_{surface}) \cdot e^{-1}$$

- P_2: pressure at which the integrated value correspond to 50% of the TPW

- P_3: Average pressure weigthted with the layer specific humidity $P_3 = \sum_i \frac{p(i) \cdot q(i)}{q(i)}$

Figure 5 shows an example (WMO station #94120, Darwin) of time series for normalized radiosonde derived variables: surface pressure, TPW, CAPE, SFC mixing ratio.

Table 1 reports the information (identification, geographical coordinates, altitude and number of valid soundings) on the 45 selected radiosonde sites. **Figure 6** shows the geographical position of the radiosonde sites analysed as well as a classification based on the occurrence of a relatively significant spectral component of period 13.5-14.5 days, 27.5-28.5 days or both. Upper panel (TPW), middle panel (SFC water vapour mixing ratio), lower panel (CAPE)

Table 1. Selected WMO Radiosonde sites

| ID	WMO #	Name	Lat °N	Lon °E	Elevation slm	Soundings
IN	43333	PORT BLAIR	11.67	92.72	79	19356
TH	48455	BANGKOK	13.73	100.57	20	19550
TH	48565	PHUKET/MAI KHAO	8.100	98.30	3	6497
TH	48568	SONGKHLA	7.200	100.6	4	18165
MY	48601	PENANG/BAYAN LEPAS	5.300	100.270	3	29756
MY	48615	KOTA BHARU	6.170	102.280	5	26650
MY	48657	KUANTAN	3.780	103.220	18	23982
SN	48698	SINGAPORE/CHANGI	1.370	103.980	3	26477
VM	48900	HO CHI MINH	10.82	106.670	10	18677
GQ	91212	AGANA	13.48	144.8	78	31448
FM	91334	CHUUK	7.470	151.850	3	20760
PS	91408	KOROR	7.330	134.480	30	21141
FM	91413	YAP	9.480	138.080	14	20926
PP	92035	PORT MORESBY	-9.380	147.220	58	4160
PP	92044	MOMOTE	-2.070	147.430	5	7082
PP	94014	MADANG	-5.220	145.8	6	730
AS	94120	DARWIN	-12.43	130.870	29	24657
AS	94150	GOVE AIRPORT	-12.28	136.820	53	10129
AS	94170	WEIPA AIRPORT	-12.68	141.920	22	7734
AS	94175	THURSDAY ISLAND	-10.58	142.220	58	234
ID	96011	BANDA ATJEH/BLANGBINTANG	5.520	95.42	21	139
ID	96035	MEDAN/POLONIA	3.570	98.68	25	12605
ID	96147	RANAI NATUNA BESAR	3.950	108.380	2	4326
ID	96163	PADANA TABING	-0.880	100.350	3	9126
ID	96237	PANGKALPINANG	-2.170	106.130	33	8140
BX	96315	BRUNEI AIRPORT	4.930	114.930	15	17315
MY	96413	KUCHING	1.480	110.330	27	22402
MY	96441	BINTULU	3.200	113.030	5	18269
MY	96471	KOTA KINABALU	5.950	116.050	3	25528
MY	96481	TAWAU	4.270	117.870	20	16700
ID	96749	SOEKARNO	-6.120	106.650	8	11247
ID	96933	SUBABAJA/PERAK	-7.220	112.720	3	1168
ID	96935	SURABAJA	-7.370	112.770	3	10541
CK	96996	COCOS ISLAND	-12.18	96.83	4	17984
ID	97014	MENADO/MAPANGET	1.530	124.920	80	12364
ID	97072	PALU/MUTIARA	-0.6800	119.730	86	9220
ID	97180	MAKASSAR	-5.070	119.550	14	13371
ID	97372	KUPANG PENFUI	-10.17	123.670	138	9329
ID	97502	SORONG	-0.9300	131.120	2	327
ID	97560	BIAK/MOKMER	-1.180	136.120	11	10048
ID	97724	AMBON	-3.700	128.080	12	6751
ID	97980	MERAUKE	-8.470	140.380	3	5373
RP	98444	LEGASPI	13.13	123.730	17	4631
RP	98618	PUERTO PRINCESA	9.750	118.730	15	2380
RP	98753	DAVAO AIRPORT	7.120	125.650	25	2377
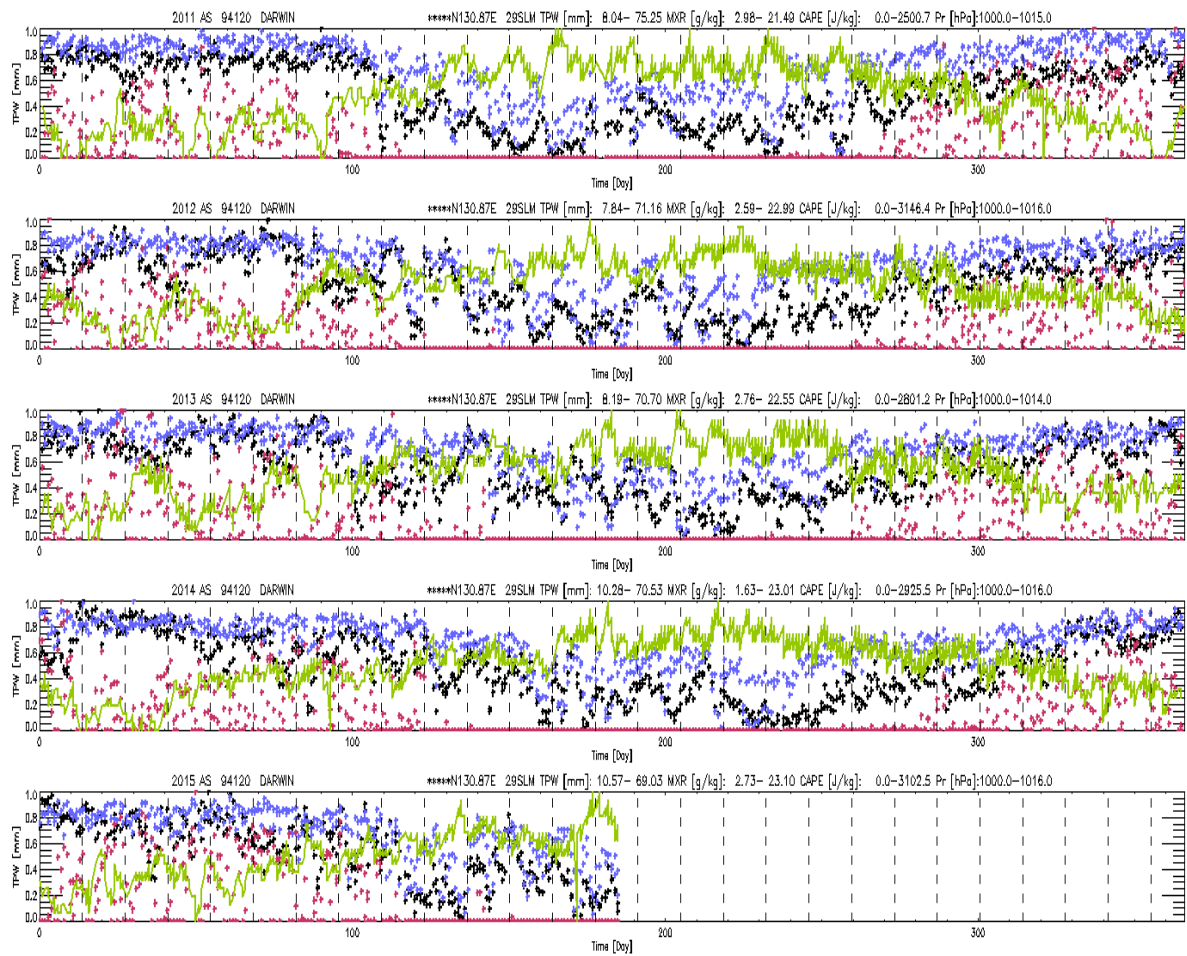
Figure 5. Example (WMO station #94120, Darwin) of time series for radiosonde derived variables (Green: surface pressure, Black: TPW, Red: CAPE, Blue: SFC mixing ratio). The values are normalized, max and min for each variable is reported in the title of each panel. Dashed vertical lines are plotted every 13.66 days.
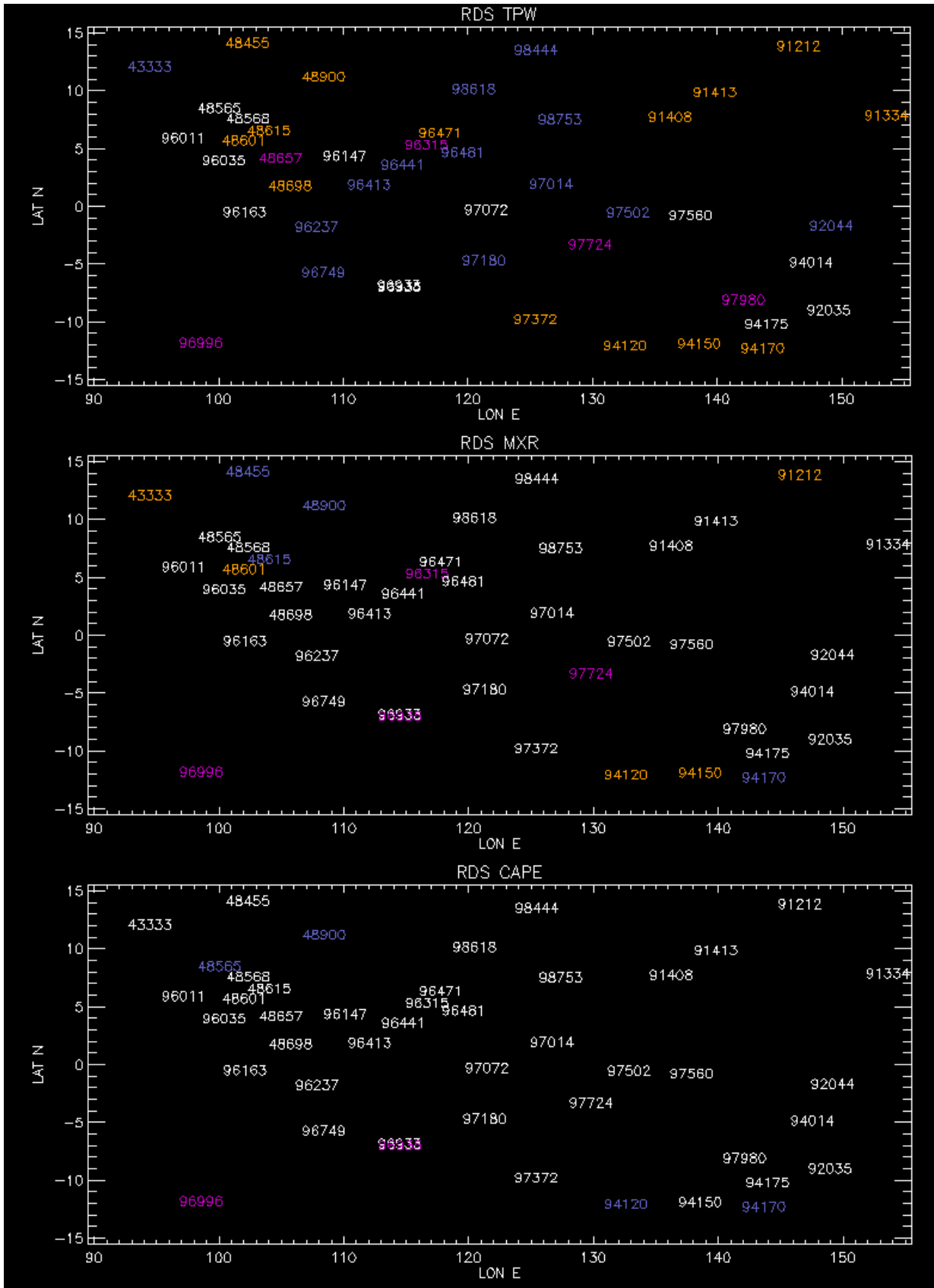
12

Figure. 6 Geographical distribution of the radiosonde sites analysed (WMO code reported). The color different than white indicates the occurrence of a not negligible spectral component of period 13.5-14.5 (magenta), 27.5-28.5 (blue) or both (orange). Upper panel (TPW), middle panel (SFC water vapour mixing ratio), lower panel (CAPE).

2.3 In situ Water Pressure and Temperature Data

An array of shallow pressure, temperature and salinity sensors was deployed to monitor the flow of the water from the Pacific Ocean as it exits the interior Indonesian seas into the Indian Ocean (Chong et al., 2000). Nine subsurface pressure gauges, equipped with temperature and conductivity (salinity) sensors, were deployed in the five major outflow passages along the Indonesian archipelago as part of a joint U.S. – Indonesian program in 1995-1999 (Sprintall et al., 2003) and again in 2003-2006 as part of the INSTANT program (http://www.ldeo.columbia.edu/res/div/ocp/projects/instant/projectDescription.html) (Sprintall et al., 2004), although gaps exist due to instrumental failure at some sites during both programs. Pressure was measured every 3 min by the Paroscientific quartz sensor with an accuracy of 0.3 mbar. The largest error comes from instrument drift, estimated to decrease 0.3 mbar every year (Wearn and Larson, 1982), a relatively small error compared to the dynamic signal of O(10 mb). The Seabird SBE-04 temperature-conductivity sensor has a manufacturer specifications of O(0.001°C) accuracy in temperature and O(0.003) in salinity.

Pressure gauge pairs were deployed so as to span a passage (**Figure 7**) and give a corresponding pressure (essentially sea level) gradient in order to compute shallow geostrophic velocity and transport (Hautala et al., 2001). Here the observational temperature and pressure time series are averaged to 0.5 hour resolution and examined for tidal mixing signatures. The pressure gauges and their accompanying CTD sensors were diver deployed just offshore of the bounding islands in each strait at a depth of 5-8 m. As such, the gauge depth is not truly a measure of SST, however typically the water column is well-mixed in the near-shore environment and so can be considered representative of a bulk SST measurement. In addition, these directly observed temperature measurements provide records of the near coastal conditions that are missing in the remotely sensed measurements. The gauges are located on the islands of Bali and Lombok (Lombok Strait); Sumbawa and North Sumba (Sumba Strait); South Sumba and Roti (Savu Strait); North Ombai and South Ombai (Ombai Strait); and Roti and Ashmore Reef (Timor Passage). **Figure 8** shows an example of time series of the 3 measured variables for the site of Sumbawa.
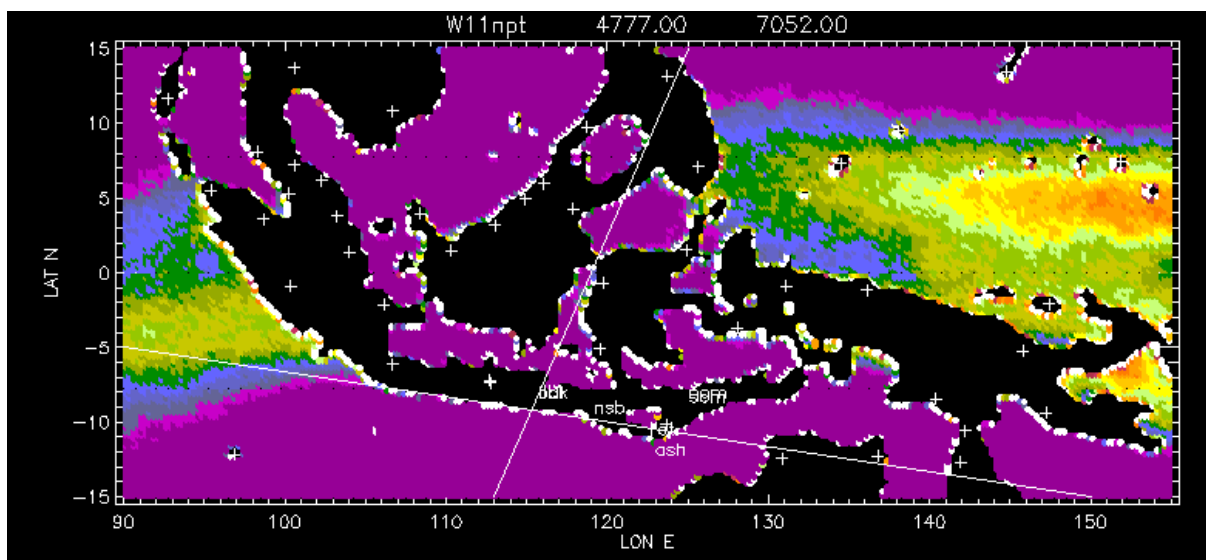

Figure 7. Position of the buoys. Also reported as a background map the NPT for the surface wind (W11) with the 10.8 GHz channel as (figs 2-4) as well as the position (crosses) of the radiosonde sites.
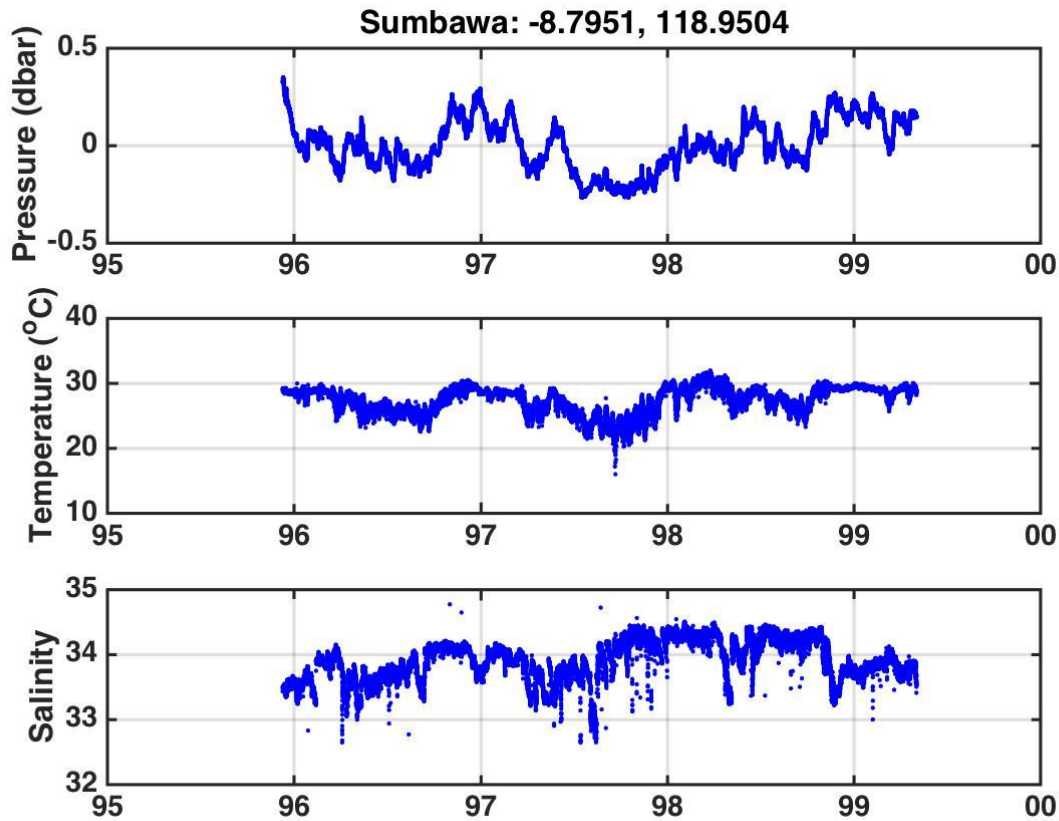
Figure 8 Example of time series of the 3 measured variables for the site of Sumbawa.

2.4 Other candidate datasets

Radiosonde from the Automated Shipboard Aerological Programme (ASAP). Even if most of the radiosonde sites are located on the coast, the influence of tidal mixing may be not evident in the time series of such sites because of the influence in the lower layers of WV derived from land surface-atmosphere exchange processes. For this reason we considered an additional dataset of operational radiosondes launched from ships. The ship based soundings are from the Automated Shipboard Aerological Programme (ASAP, www.jcommops.org/sot/asap/) and they were obtained through the Meteorological Archival and Retrieval System (MARS www.ecmwf.int/services/archive/) at the European Centre for Medium-Range Weather Forecasts (ECMWF). Even if, for such type of measurements with a changing position it is not possible to perform a time series analyses it could be of interest, at least to analyze observations in proximity of a land based operational site to document the differences between land and ocean based vertical distribution of WV. **Figure 9** shows the geographical distribution of available ASAP soundings for the period: 1979-2014. As evident from the image there are very few measurements in the study area, in particular in the internal Seas and in Indian Ocean side, therefore the analyses of this dataset has not been carried out.
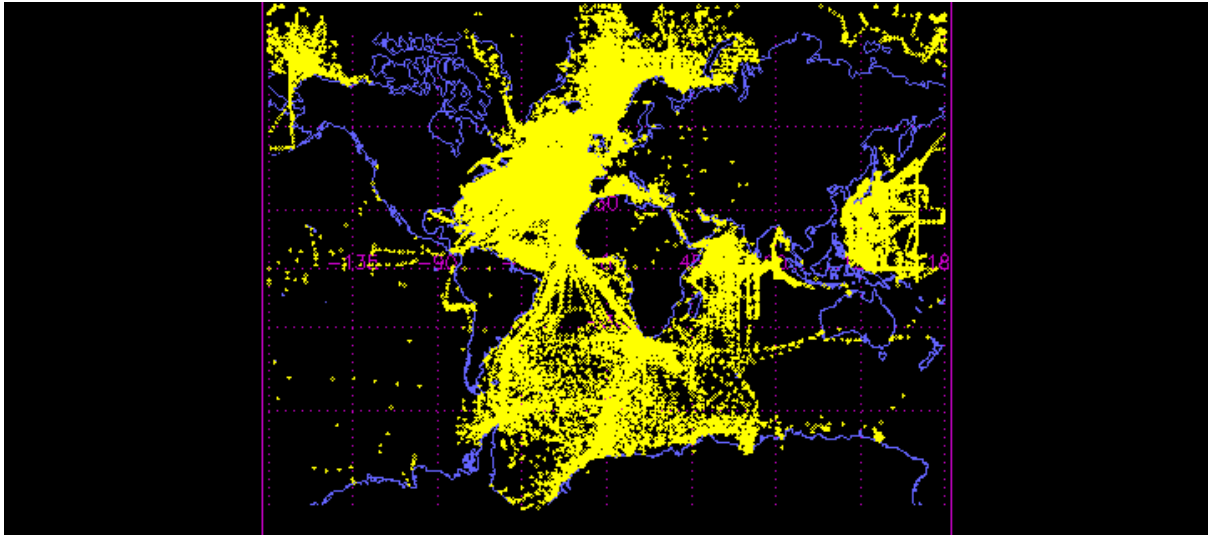
Figure 9 Geographical distribution of available ASAP soundings for the period: 1979-2014.

3   Methodology and challenges

Our approach will be:
1. to investigate if there are periodicities in the time series induced by some factor (e.g. temporal sampling) related to the measurement technique. This will be done by analyzing the documentation relative to each measurement technique and by comparing when possible independent sources of information. In particular, TMI derived SST will be compared against buoys measurements, and TMI derived TPW against radiosonde estimates.
2. to look for periodicities likely to be related to ocean tides in the existing in situ (Radiosonde & Buoys) data sets.
3. to extend the spectral analysis to TMI derived products and to interpret the spatial distribution of the results

In this subsection we discuss the challenges that we expect to face when trying to describe quantitatively the atmospheric response to the tidal mixing in the Indonesian Seas.
1. **Figure 10** (upper panel) shows the amplitude of Mf from TPX7.2 model in the area of interest. As a reference the M2 amplitude map is also reported (lower panel). Note that the Mf amplitude is about two order of magnitude less than the M2 one. On the other hand, the spatial distribution is not the same, and another relevant factor is the fact that an intense but short disturbance (M2) in the SST may, because of the thermal inertia of the atmosphere, have less effect of a less intense but slower perturbation (Mf). These temperature variations appear to be due to nonlinear dynamics, which cause a redistribution of tidal energy from semi-diurnal and diurnal to fortnightly and longer periods.
2. Is the atmospheric signal contaminated by other forcing than the tidal one?
3. Cannot assume the atmosphere is responding in a 1D sense to the SST patterns at the same place and time. Potentially local SST changes can have an impact on atmospheric changes at another location.
4. For a tidal mechanism of SST variability to be plausible, it must be shown that tide raising forces generate, and therefore dissipate, enough energy in mixing ocean water to compete with other mixing mechanisms.

5. Need to make sure that sampling is not affecting signal. Use many cross-verifications to show this. But for example, the Shallow Pressure Gauge Array (SPGA) buoys agree in spatial distribution with SST, no strange artifacts in satellite data – tend to agree with buoys and radiosondes.
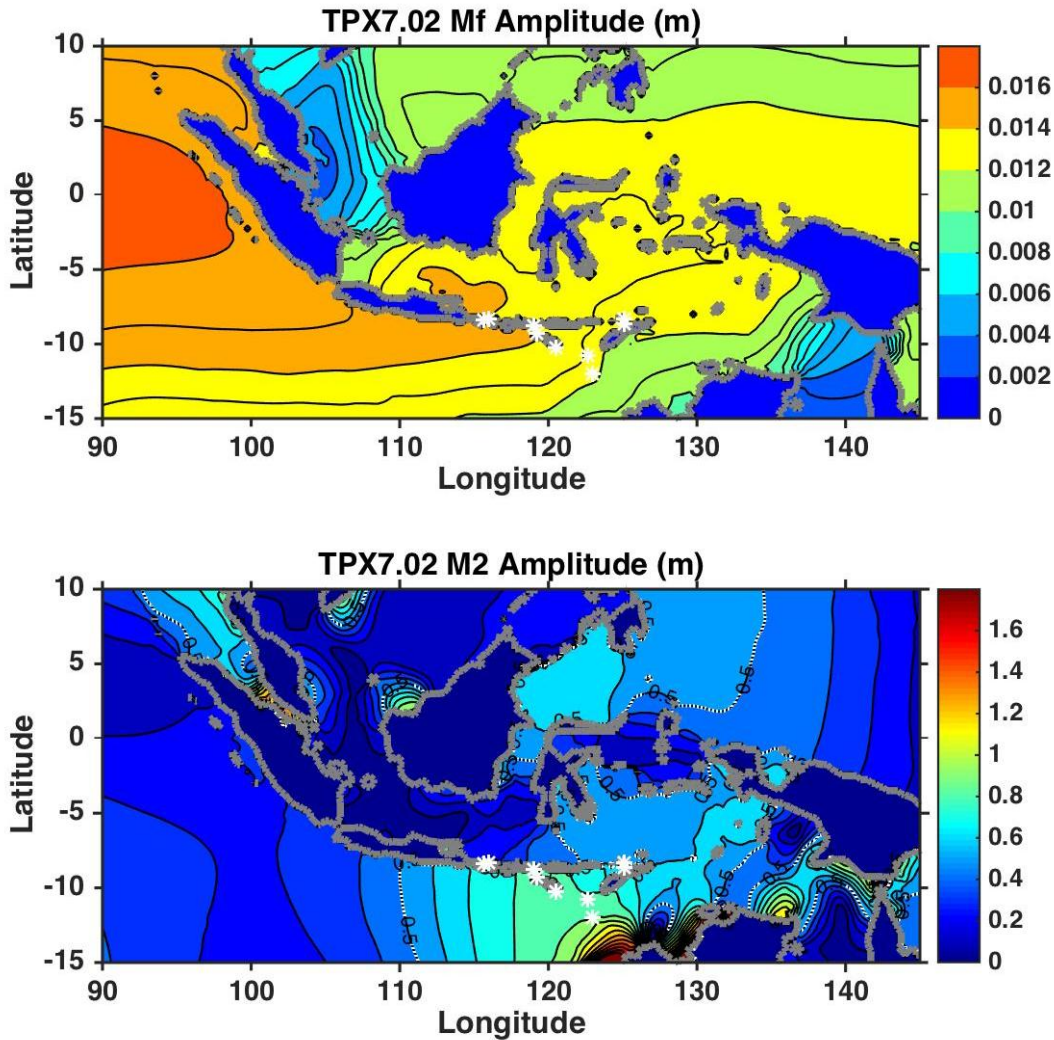

Figure 10: The amplitude (m) of the (upper panel) Lunar Fortnightly (Mf) and (lower panel) M2 tides from the TPX7.2 tidal model for the Indonesian seas. White asterisks show the location of the *in situ* temperature measurements referred to in the text.

4 Results

Match-up

A preliminary set of analysis consists simply in plotting time series of all possible combinations of variables observed by satellite, buoy and radiosonde approximately in the same geographical position. This very qualitative type of analysis is aimed to identify inconsistency between the overall behavior of the different measurements that could be due to instrument/sampling related artifact (i.e. solar radiation effects in radiosondes).

4.1.1 TMI-RDS (TPW)

Figure XXXX shows an example of comparison TMI-RDS plotting the annual time series of
SST from the buoy site and from a max of 3 corresponding TMI sites:
- closest one,
- closest one with at least 1000 observations (including rain contaminated ones)
- the one having the largest number of observations (including rain contaminated ones) within
a max distance radius of 200 km
If the above characteristics are found in a single site the time series reported in the figure has
the colour of the last in the list. A set of similar plot was produced and analysed qualitatively.
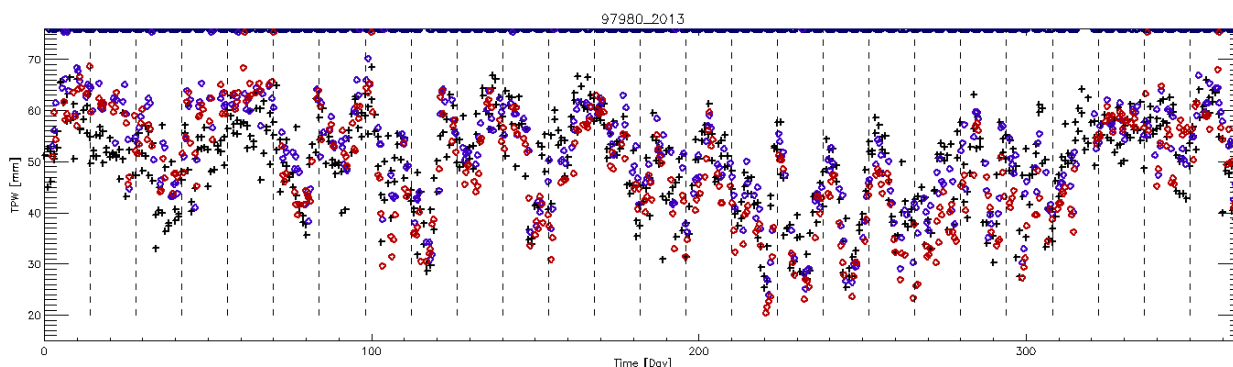

Fig.XXX. Example of comparison TMI-RDS (WMO site #97980) plotting the annual (2013) time series of
TPW from the radiosonde site (+) and from a max of 3 corresponding TMI sites (◊):(black) the closest one,
(blue) the closest one with at least 1000 observations (including rain contaminated ones), (red) the one within a
max distance radius of 200 km having the largest number of observations (including rain contaminated
ones).TMI measurements at about 35°C are the one contaminated by the precipitation. Dashed lines are plotted
every 13.66 day as a period of interest for tidal derived signal.

RESULTS_USED\RDS\MATCHUP_RDS\
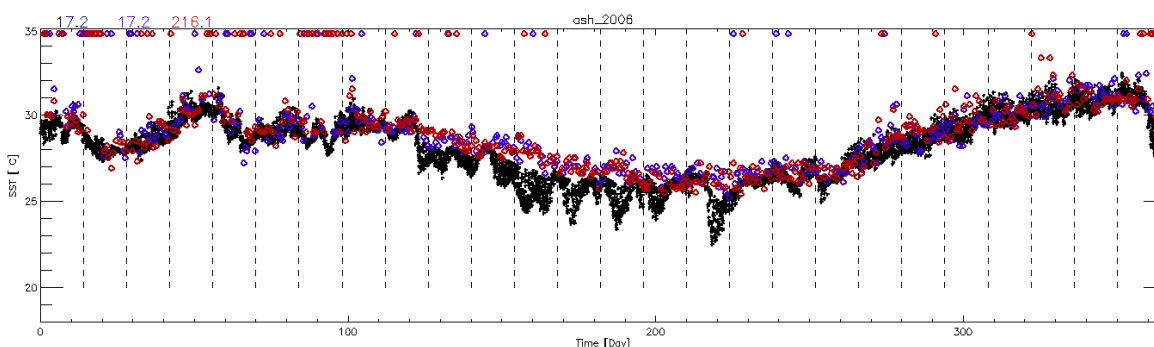
4.1.2 TMI-Buoys (SST)

Fig.XXX. Example of comparison TMI-BUOY (ASH) plotting the annual (1998) time series of SST from the buoy site (+)
and from a max of 3 corresponding TMI sites (◊):(black) the closest one, (blue) the closest one with at least 1000
observations (including rain contaminated ones), (red) the one within a max distance radius of 200 km having the largest
number of observations (including rain contaminated ones) Also reported, with the same colour code, the distance between
the buoy and the TMI gridbox

18

4.1.3 TMI-Buoys (TPW)

The last consistency test was performed by comparing the buoys SST against the RDS TPW.
For each buoy the closest RDS site was searched the following table reports
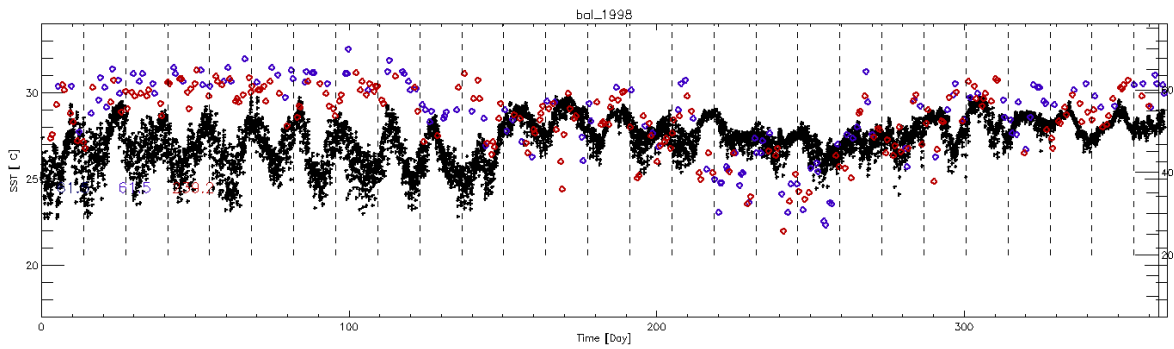
4.1.4 RDS-Buoy (TPW-SST)

Buoy	RDS WMO#	Buoy Lat N°	Buoy Lon E°	RDS Lat N°	RDS Lat N°	Distance [Km]
ash	97372	-12.22	123.00	-10.17	123.67	239.62
bal	96935	-8.40	115.71	-7.37	112.77	343.93
lbk	96935	-8.35	116.04	-7.37	112.77	376.65
nom	97372	-8.35	125.07	-10.17	123.67	254.40
nsb	97180	-9.38	119.20	-5.07	119.55	481.52
rot	97372	-10.81	122.68	-10.17	123.67	**129.82**
som	97372	-8.66	125.11	-10.17	123.67	230.42
ssb	97372	-10.25	120.52	-10.17	123.67	345.32
swa	97180	-8.80	118.95	-5.07	119.55	419.91

Single site spectral analysis

4.1.5 Radiosondes

The spectral analysis of the time series for all radiosonde derived variables
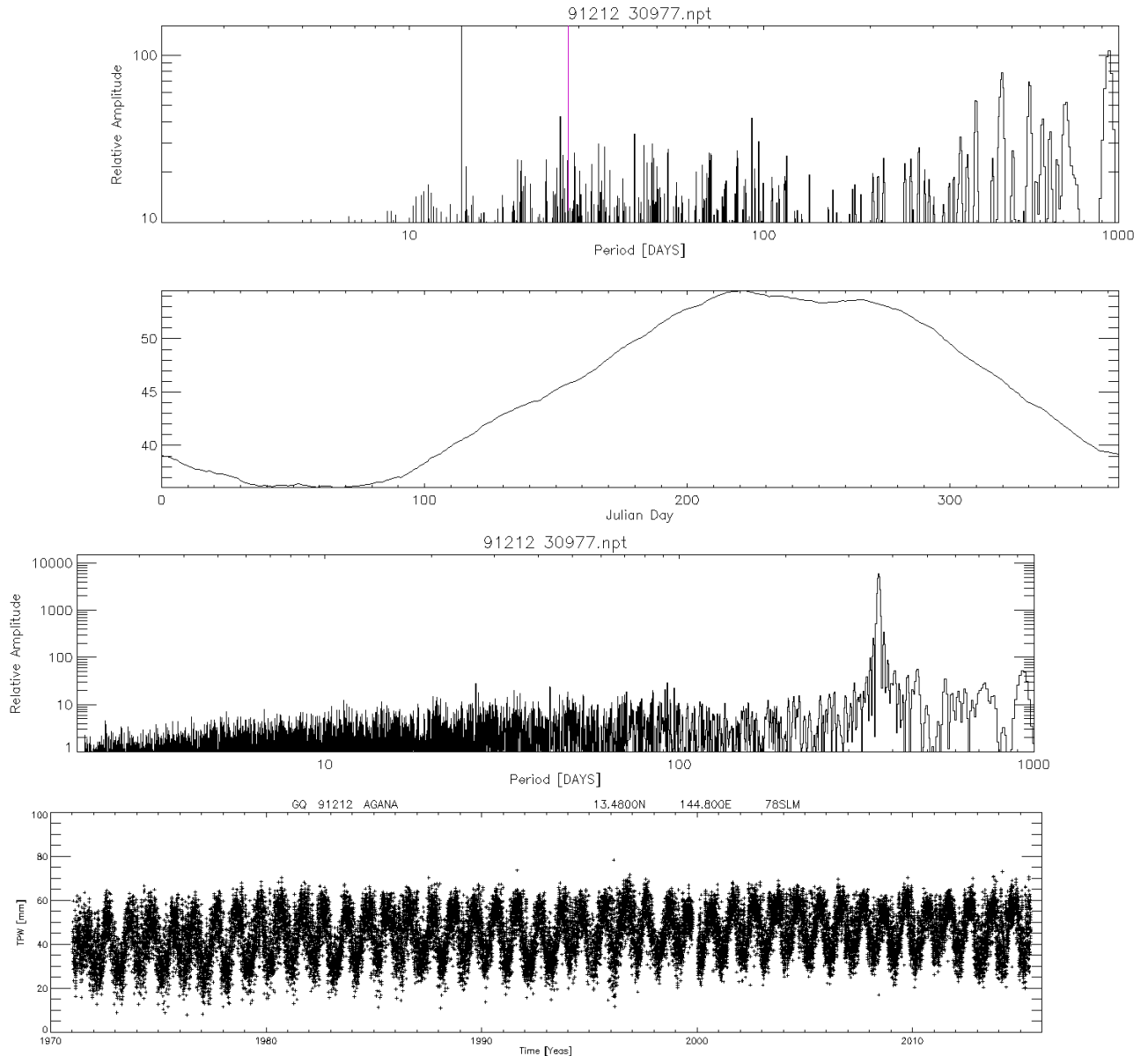

Example of results of spectral analysis of the TPW time series for WMO site 91212. From bottom to upper panel: Time series, spectral analysis, average annual cycle, spectral analysis of the time series once removed the average annual cycle

From the analyses of the time series it looks like there is some 14 days periodicity evident during the dry season.
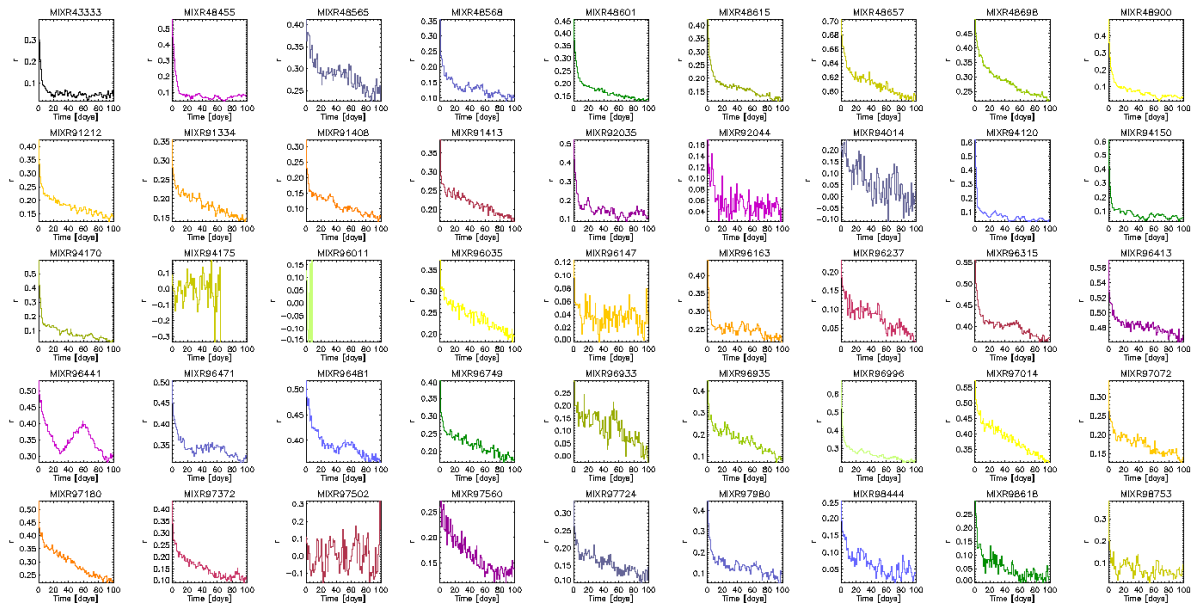
Fig.XXXX Correlogram Surface mixing ratio (RDS\)
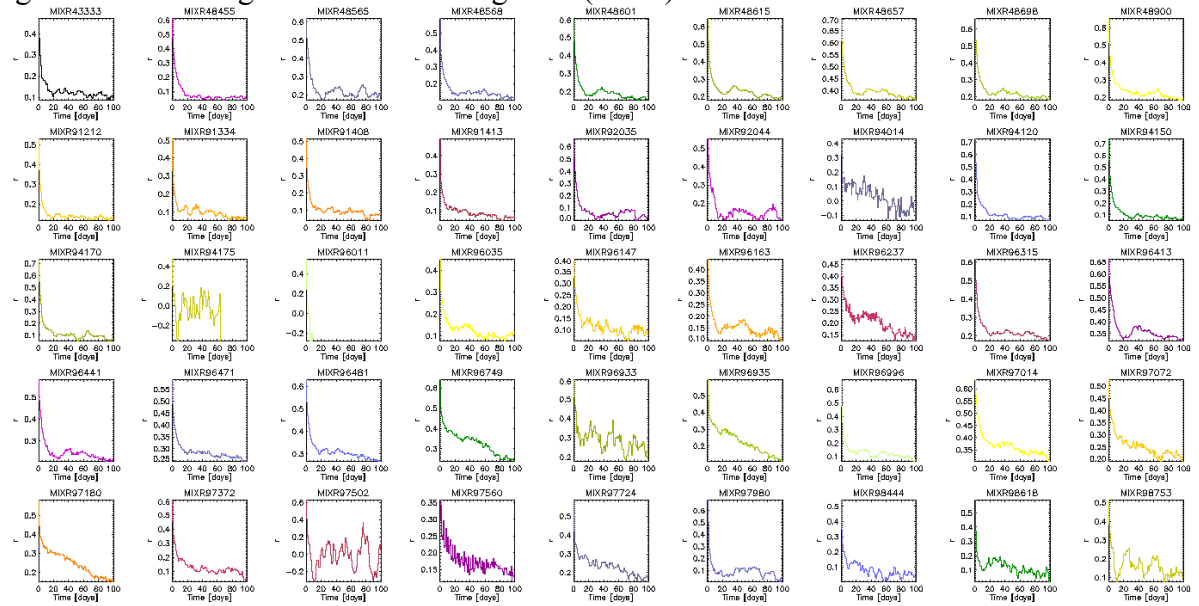
Fig.XXXX Correlogram TPW (RDS\)

4.1.6 Buoys

Table X: Maximum amplitude (°C) of the spring-neap temperature signal from the SST array in the Indonesian Seas. The period represents the closest period to the MSf and Mf frequencies. This will then show how this amplitude changes with the annual cycle.

Gauge	MSf (14.765days)		Mf (13.66days)	
All Periods	Amp	period	amp	Period
Lombok	0.0942	14.77	0.0903	13.63
Bali	0.6155	14.76	0.1313	13.66
Ashmore	0.0781	14.68	0.0518	13.66
Roti	0.1661	14.76	0.0462	13.97

NorthOmbai	0.8449	14.77	0.3293	13.66
SouthOmbai	0.5562	14.76	0.2089	13.66
Sumbawa	0.2926	14.77	0.1235	13.62
NorthSumba	0.2691	14.78	0.0790	13.97
SouthSumba	0.0545	14.93	0.1098	13.94

1995-1999	Amp	Period	amp	period
Lombok	0.0808	14.79	0.0877	13.64
Bali	0.6364	14.77	0.1578	13.67
Ashmore	0.0878	14.64	0.0661	13.63
Roti	0.1711	14.77	0.0395	13.79
NorthOmbai	0.9425	14.76	0.3499	13.65
SouthOmbai	0.5488	14.77	0.1589	13.66
Sumbawa	0.2926	14.77	0.1235	13.62
NorthSumba	0.2691	14.78	0.0790	13.97
SouthSumba	0.0545	14.93	0.1098	13.94

2003-2006	Amp	Period	amp	period
Lombok	0.1916	14.63	0.1612	14.00
Bali	0.6081	14.75	0.1074	13.71
Ashmore	0.1011	14.73	0.0771	13.50
Roti	0.1657	14.79	0.0828	13.98
NorthOmbai	0.7505	14.76	0.3092	13.67
SouthOmbai	0.5726	14.76	0.2679	13.67

alysis 2a: Spatial spectral analysis: overall period.
Analysis 2b: Spatial spectral analysis: single year.

Results

Figure 3: GHR-SST results from Susan Wijffels shows small signal (0.1°C) focused around the narrow passages between islands

SPGA – not contains many tidal signals. Need to isolate the Mf. Perhaps also use the p-time series as in Ffield and Gordon (1996). Perhaps show example of raw data to illustrate this.

Table 1: SPGA shows much larger amplitude. Up to ~ 1 °C in Ombai Strait. Much regional variability.

Atmospheric Response:

for atmosphere, not a huge signal but still present.

Shows in time series more than spectra.

More signal in dry season than wet season

Annual and semi-annual signal dominate so may need to isolate a shorter period to examine signal (e.g. 4 months)

Removed low frequency but still noisy and aliasing back in to higher frequency in WV

Did spectra for year-to-year chunks – need to show this every year, or averaging which successfully derived the signal in SST in the straits, but not WV. Except in Arafura Sea where the signal is strong and this may be a region of interest (amphidromic tidal point). Not a lot happening in the Banda Sea (contradicts Ffield and Gordon).

Constructed sections along Nusa Tengarra islands (Sumatra-Java-Bali- Timor); 90°E; from Sumatra-Sulawesi-Pacific; but signal not always consistent or strong – probably needs fine tuning.

Constructed boxes near SPGA buoys and examined remotely sensed data either as a function of proximity to buoys, or number of points

Will a 2°C SST change 10 ml WV? Yes! But need to change the scale8 of the WV. Seems like E cannot do this alone.

5 Summary and Discussion

Question is whether the signal is due to any artifact in the measurement or additional influence?

lunar atmospheric tide influence? Is WV changing because of SST or because of lunar atmospheric tide?

Are the model improvements because of the tidal mixing or because they cannot represent atmospheric tidal mixing? Are they just representing this process in their models?

How do we get at this? Can we address this through an order of magnitude calculation?

SST-WV/scale8 diagrams- look at CAPE values or direction of wind when you get the driest or wettest air masses that may affect the relationship.

Important to bear in mind that the SST response to tidal mixing might not be a localized phenomena but the impact of tidal mixing may be spread either because of different tidal generation/dissipation sites (Nagai and Hibiya, 2015) or through advective processes related to the wind-driven circulation (Kida and Wijffels, 2012). The relatively local increase in mixing can involve far reaching remote effects.

Perform the spectral analysis of the variables linked to the vertical distributionof the WV.

Document interannual variability – relationship to ENSO or IOD or large monsoon year or year when M2/S2 interaction big because of low-frequency tidal interaction.

Answer science questions raised in Introduction

Implications for future research

Concerning the analyses performed on the radiosonde dataset, as mentioned in the section describing the dataset, only a criterion on the minimum number of levels (5) was applied to create the time series. Other Q/C criteria, regarding for example the uppermost layer included in the integral (e.g. Liberti et al. 2012), and an objective

Consistency of the information contained in each analysed dataset was verified. Periodicities introduces by instrument/sampling issue(s) are either negligible or identified and characterized as for the combination of diurnal cycle and TMI sampling producing a components at about 23 and 48 days.

There is a large spatial variability of the results that may be explained as a combined effect of the geographical complexity of the region that induces multiscale interactions among ocean and atmosphere processes. The spatial representation of the results is one of the objective of this study and should be improved.

We also found a temporal dependence that in the most common case means that during the dry season a periodicity of 14 days is evident in the TPW time series. This results can be explained with the fact that during moist periods, such as the monsoon in the tropics, the effect is not evident because the atmosphere is already saturated by the water vapour that characterize the wet monsoon season. As a consequence the analyses should focus on the dry season.

For subset (spatial and temporal) of the datasets we found a 13-14 days components both in the SST as well as in TPWV. In some cases, for Ex ... they are in opposite phase: THIS CAN BE EXPLAINED Assuming the observed 13-14 periodicities are real both in the atmosphere as in the ocean an open question is if the observed signal in the atmosphere is a response to the SST variation due to tidal mixing or if it is just the effect of the lunar atmospheric tides (SEE REFS).

A first question we can try to answer is how large can be the change in TPW in response to a 2-3 K amplitude of the tidal mixing cycle amplitude. If an SST of the order of magnitude of the expected amplitude cannot change significantly the TPW value then we can exclude that occurence of a TPW 13-14 cycle can be due to a response to a change in the SST.

In order to test this hypothesis we compare some climatological relationship linking SST and TPW to the observed behaviour from the TMI data. Few considerations:

- we apply the functional form suggested by Stephens (1990).

.

$$TPW = 10.82 \cdot \left(\frac{RH_{sfc}}{1 + \lambda} \right) \cdot e^{\; a(SST-288)}$$

More recent literature (e.g. Zhang & Qiu 2008, Kanemaru & Masunaga, 2013).suggests other functional forms but the main difference is to introduce the spatial and temporal dependence of the parameters in the formula

- the formula is based on 3 parameters: a) the atmospheric scale height (basically due to the hydrostatic equation) that depends from the air density (i.e. from the temperature) and we assumed a fixed value of 9 km. b) the relative humidity at surface (the colour of the line) that we set to 75% (red=dry) or 95% (wet=blue) c) the water vapour scale height set to 1 (full line),2 (dots),3 (dashed) km.

Each panel is one year for a given grid box. We decide to represents satellite data with a line connecting all valid observations to have somehow the information on temporal variability. Two measurements can be separated by a minimum of 12 hours to few days if there are days with precipitation. We can conclude that a change of SST of 2 degrees C keeping all parameters fixed (i.e. moving on a curve that is not physically realistic) can already produce a

change in TPW of the order of 10 mm. If we assume that a change in the WV scale height is associated with the SST change then we can get larger variations. Please note that the plotted relationships are climatological, sort of equilibrium, relationships. The realistic response could be either larger if the increase of SST corresponds to a relatively instantaneous response of the atmosphere giving a change of water vapour scale height or smaller because of the thermal inertia of the atmosphere. Because this region is subject to convection it may be realistic to imagine a fast response of the atmosphere.
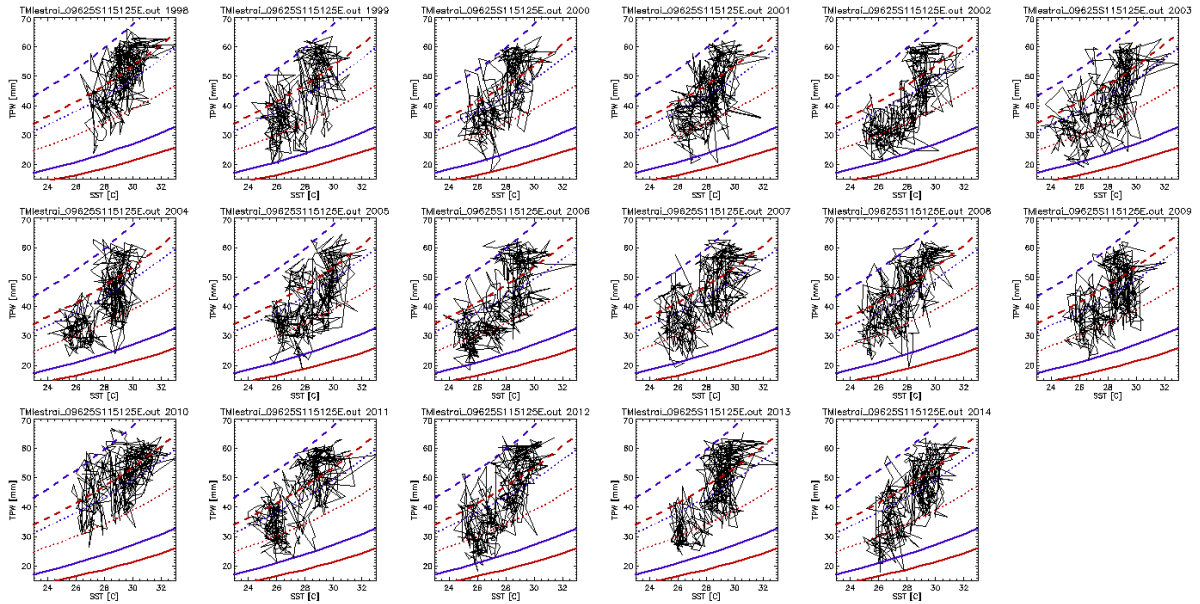

Fig.XXX. Examples of annual cycles (bos 6.25°S-115.125°E) of relationship between SST and TPW. Plotted lines

Appendix 1: Common colour scale

References

Alford, M., Gregg, M., Ilyas, M., (1999). Diapycnal mixing in the Banda Sea: Results of the first microstructure measurements in the Indonesian Throughflow. *Geophysical Research Letters*, 26, 2741–2744.

Antonov, J.I., Seidov, D., Boyer, T.P., Locarnini, R.A., Mishonov, A.V., Garcia, H.E., Baranova, O.K., Zweng, M.M. & Johnson, D.R. (2010) *World Ocean Atlas 2009, Volume 2: Salinity.* S. Levitus, Ed. NOAA Atlas NESDIS 69, U.S. Government Printing Office, Washington, D.C. 184 pp.

Anyamba, E., E. Williams, J. Susskind, A. Fraser-Smith, and M. Fullekrug (2000), The manifestation of the Madden-Julian Oscillation in global deep convection and in the Schumann resonance intensity, *J. Atmos. Sci.*, 57, 1029–1044.

Brierley, C. M., and A. V. Fedorov. Tidal mixing around Indonesia and the Maritime continent: Implications for paleoclimate simulations. *Geophysical Research Letters* 38.24 (2011).

Chong, J., J. Sprintall, S. Hautala, W. Morawitz, N. Bray and W. Pandoe, 2000: Shallow throughflow variability in the outflow straits of Indonesia. *Geophys. Res. Letts.* 27, 125- 128.

Durre,I,, R.S.Vose & D.B.Wuertz, (2006) Overview of the Integrated Global Radiosonde Archive". J. of Climate, 19, 1, 53-68.

Ffield, A., & A. L. Gordon (1992). Vertical Mixing in the Indonesian Thermocline, J. Phys. Oceanogr., 22, 184-195.

Ffield, A., & A.L: Gordon, (1996) Tidal mixing signatures in the Indonesian Seas. J. Phys Oceanogr. 26, 1924-1937.Ffield, A., K. Vranes, A. L. Gordon, R. D. Susanto and S. L. Garzoli, 2000: Temperature Variability within Makassar Strait, *Geophys. Res. Lett.* 27: 237-240.

Ffield, A., and R. Robertson, 2005: Indonesian Seas: Finestructure variability. *Oceanography,* 18, 108–111.

Graham, NE, Barnett TP., 1987. Sea-Surface Temperature, Surface Wind Divergence, and Convection over Tropical Oceans, *Science.* 238:657-659.

Hatayama, T. 2004. Transformation of the Indonesian throughflow water by vertical mixing and its relation to tidally generated internal waves. *Journal of Oceanography* 60:569-585.

Hautala, S., J. Reid, and N. Bray. 1996. The distribution and mixing of Pacific water masses in the Indonesian seas. *Journal of Geophysical Research* 101:12,375–12,389.

Hautala, S., J. Sprintall, J. T. Potemra, J. C. Chong, W. Pandoe, N. Bray, and A. Ilahude, 2001: Velocity structure and transport of the Indonesian Throughflow in the major straits restricting flow into the Indian Ocean. *J. Geophys. Res.,* 106, 19 527– 19 546.

Jochum, M., & Potemra, J.T. Sensitivity of tropical rainfall to Banda Sea diffusivity in the Community Climate System Model. *J. Climate*, 21, 6445–6454 (2008)

Keeling, C. D. and T. P. Whorf, Possible forcing of global temperature by the oceanic tides, *Proc. Natl. Acad. Sci. USA,* 94, 8321–8328, 1997.

Kida, S., & S.E.Wijffels, (2012) The impact of the Indonesian throughflow and tidal mixing on the summertime sea surface temperature in the western Indonesian seas. *J. Geophys. Res*. 117, C09007.

Koch-Larrouy, A., Madec, G., Bouruet-Aubertot, P., Gerkema, T., Bessieres, L., & Molcard, R. On the transformation of Pacific Water into Indonesian Throughflow Water by internal tidal mixing. *Geophys. Res. Lett.,* 34, (2007)

Koch-Larrouy A., Madec, G., Iudicone, D., Molcard, R. & Atmadipoera, A., Physical processes contributing in the water mass transformation of the Indonesian ThroughFlow, *Ocean Dynamics*, (2008)

Koch-Larrouy, A., Lengaigne, M., Terray, P., Madec, G. & Masson, S. Tidal mixing in the Indonesian Seas and its effect on the tropical climate system, *Climate Dynamics,* 34: 6, 891 – 904, (2010)

Koch-Larrouy, A., A. Atmadipoera, P. van Beek, G. Madec, J. Aucan, F. Lyard, J. Grelet, and M. Souhaut (2015). Estimate of tidal mixing in the Indonesian archipelago from multidisciplinary data, *Deep-sea Res.*, 106, 136–153.

Li G., H.Zong & Q.Zhang (2011) 27.3-day and Average 13.6-day Periodic Oscillations in the Earth's Rotation Rate and Atmospheric Pressure Fields Due to Celestial Gravitation Forcing. ADVANCES IN ATMOSPHERIC SCIENCES, VOL. 28, NO. 1, 2011, 45–58

Liberti, G.L., Buzzicotti, M. & C.Transerici, (2012). Validation of TMI derived Total Precipitable Water Vapour with operational soundings. Proc. Microrad 2012. Frascati, Italy. 4pp.

Loder J.W. and Garrett C. 1978. The 18.6-year cycle of sea surface temperature in shallow seas due to variation in tidal mixing. *J. Geophys. Res.,* 83: 1967–1970.

McKinnell S.M. and Crawford W.R. 2007. The 18.6-year lunar nodal cycle and surface temperature variability in the northeast Pacific. *J. Geophys. Res.,* 112: C02002, DOI: 10.1029/2006JC003671

NIMA: Department of Defense World Geodetic System 1984, Tech. Rep. 3rd Edition TR8350.2, 2000. 175 pp. Available at: earth-info.nga.mil/GandG/publications/tr8350.2/wgs84fin.pdf

Nagai, T. and T. Hibiya, 2015, Internal tides and associated vertical mixing in the Indonesian Archipelago, *J. Geophysical Research*, doi: 10.1002/2014JC010592

Press, W. H., S. A. Teukolsky, W. T. Vetterling, and B. P. Flannery, Numerical Recipes in FORTRAN, The Art of Scientific Computing, 965 pp., Cambridge Univ. Press, New York, 1992.

Qu, T., Y. Du, J. Strachan, G. Meyers, and J. Slingo, 2005: Sea surface temperature and its variability in the Indonesian region. *Oceanography*, 18 (4), 50–61.

Ray, R.D. (2007). Decadal climate variability: is there a tidal connection? *J. Climate*, 20, 3542-3560.

Reynolds, R.W., Smith, T.M., Liu, C., Chelton, D.B., Casey, K.S. & Schlax, M.G. (2007). Daily high-resolution blended analyses for sea surface temperature. *J. Climate*, 20, 5473-5496.

Reynolds, R.W., Gentemann, C.L. & Corlett, G.K. (2010). Evaluation of AATSR and TMI satellite SST data, *J. Climate*, 23, 152-165.

Robertson, R., and A. Ffield (2005), M_2 baroclinic tides in the Indonesian Seas, Oceanography, 18, 62–73.

Sajith A., et al. (2007). Evaluation of daily and diurnal signals of total precipitable water (TPW) over the Indian Ocean based on TMI retrieved 3-day composite estimates and radiosonde data. *Int. J. Climatol*. 27, 761-770.

Schiller, A. (2004), Effects of explicit tidal forcing in an OGCM on the water-mass structure and circulation in the Indonesian throughflow region, *Ocean Modell.,* 6, 31–49.

Smith, W. H. F. and D. T. Sandwell (1997), Global Seafloor Topography from Satellite Altimetry and Ship Depth Soundings, Science 277: 1956-1962

Sprintall, J., A. L. Gordon, A. Koch-Larrouy, T. Lee, J. T. Potemra, K. Pujiana, and S. E. Wijffels, 2014. The Indonesian Seas and their impact on the Coupled Ocean- Climate System. *Nature Geoscience*, doi:10.1038/ngeo2188

Sprintall, J., S. Wijffels, A. L. Gordon, A. Ffield, R. Molcard, R. D. Susanto, I. Soesilo, J. Sopaheluwakan, Y. Surachman, and H. M. van Aken (2004), INSTANT: A new international array to measure the indonesian throughflow, Eos Trans. AGU, 85, 369, doi:10.1029/ 2004EO390002

Sprintall, J., J. T. Potemra, S. L. Hautala, N. A. Bray and W. Pandoe. Temperature and salinity variability in the exit passages of the Indonesian Throughflow. *Deep Sea Res.*, 50, 2183- 2204, 2003

Stephens, G.L. (1990). On the relationship between water vapor over the oceans and sea surface temperatures. *J. Climate*, 3, 634-645.

Trenberth, K. E., J. R. Christy, and J. G. Olson (1987), Global atmospheric mass, surface pressure, and water vapor variations, *J. Geophys. Res.,* 92(D12), 14815–14826, doi:10.1029/JD092iD12p14815.

Wearn, R.B. and N.G. Larson (1982) "Measurements of the sensitivities and drift of Digiquartz pressure sensors", Deep-Sea Research, V29 (1A), 111-134

Wentz, F.J. (1997). A well calibrated ocean algorithm for special sensor microwave/imager. *J. Geophys. Res.* 102, 8703-8718.

Wentz, F.J., & Meissner, T. (2000). AMSR Ocean Algorithm, Version 2, report# 121599A-1, Remote Sensing Systems, Santa Rosa, CA, 66 pp. online at http://www.remss.com.

Wentz, F.J. & Meissner T. (2007). Supplement 1. Algorithm Theoretical Basis Document for AMSR-E Ocean Algorithm. *RSS Tech. Rpt. 051707*, Remote Sensing Systems, Santa Rosa, CA, 6 pp., Available at www.remss.com.

Wentz, F. J., C. Gentemann, D. Smith, and D. Chelton (2000), Satellite measurements of sea surface temperature through clouds, *Science*, 288, 847–850.

WMO (World Meteorological Organization), (1986) "Algorithms for Automatic Aerological Soundings" (A.H.Huper). Instruments and Observing Methods Report No. 21, WMO-TD-No. 175, Geneva.

Yasuda, I., S. Osafune, and H. Tatebe, 2006: Possible explanation linking 18.6-year nodal tidal cycle with bi-decadal variations of ocean and climate in the North Pacific. *Geophys. Res. Lett.,* 33, L08606, doi:10.1029/2005GL025237

Zhang,C. & Qiu F. 2008. Empirical Relationship between Sea Surface Temperature and Water Vapor: Improvement of the Physical Model with Remote Sensing Derived Data. *J. of Oceanography*, 64, 163-170.

Kanemaru, K. & Masunaga, H. 2013. A Satellite Study of the Relationship between Sea Surface Temperature and Column Water Vapor over Tropical and Subtropical Oceans. *J. Climate*, 26, 4204–4218